Fat fractions from high-resolution 3D radial Dixon MRI for predicting metastatic axillary lymph nodes in breast cancer patients

Thomas Winther Buus [a,*], Kim Sivesgaard [a], Tanja Linde Fris [b], Peer Michael Christiansen [b], Anders Bonde Jensen [c], Erik Morre Pedersen [a]

[a] Department of Radiology, Aarhus University Hospital, Palle Juul-Jensens Boulevard 99, 8200, Aarhus N, Denmark
[b] Department of Plastic and Breast Surgery, Aarhus University Hospital, Palle Juul-Jensens Boulevard 35, 8200, Aarhus N, Denmark
[c] Department of Oncology, Aarhus University Hospital, Palle Juul-Jensens Boulevard 99, 8200, Aarhus N, Denmark

HIGHLIGHTS

- High-Resolution 3D radial Dixon MRI allows for the creation of quantitative fat fraction images.
- Lymph node fat fractions improves diagnostic performance of MRI to detect axillary lymph node metastases.
- Lymph node fat fractions are a promising quantitative indicator of metastases in axillary lymph nodes.

ARTICLE INFO

ABSTRACT

Purpose: To assess diagnostic performance of fat fractions (FF) from high-resolution 3D radial Dixon MRI for differentiating metastatic and non-metastatic axillary lymph nodes in breast cancer patients.

Method: High-resolution 3D radial Dixon MRI was prospectively performed on 1.5 T in 70 biopsy-verified breast cancer patients. 35 patients were available for analysis with histopathologic and imaging data. FF images were calculated as fat / in-phase. Two radiologists measured lymph node FF and assessed morphological features in one ipsilateral and one contralateral lymph node in consensus. Diagnostic performance of lymph node FF and morphological criteria were compared using histopathology as reference.

Results: 22 patients had metastatic axillary lymph nodes. Mean lymph node FF were 0.20 ± 0.073, 0.31 ± 0.079, and 0.34 ± 0.15 (metastatic, non-metastatic ipsi- and non-metastatic contralateral lymph nodes, respectively). Metastatic lymph node FF were significantly lower than non-metastatic ipsi- ($p < 0.001$) and contralateral lymph nodes ($p < 0.001$). Area under the receiver operating characteristics curve for lymph node FF was 0.80 compared to 0.76 for morphological criteria ($p = 0.29$). Lymph node FF yielded sensitivity 0.91, specificity 0.69, positive predictive value (PPV) 0.83, and negative predictive value (NPV) 0.82, while morphological criteria yielded sensitivity 0.91, specificity 0.62, PPV 0.80, and NPV 0.80 ($p = 0.71$). Combining lymph node FF and morphological criteria increased diagnostic performance with sensitivity 1.00, specificity 0.67, PPV 0.86, NPV 1.00, and AUC 0.83.

Conclusions: Lymph node FF from high-resolution 3D Dixon images are a promising quantitative indicator of metastases in axillary lymph nodes.

1. Introduction

Breast cancer is the most common cancer among women and the second leading cause of cancer death [1]. The presence of axillary lymph node metastases is an important prognostic factor for overall survival [2]. The gold standard for evaluating lymph node status includes pre-operative ultrasonography (US) and fine needle aspiration of morphologically suspicious nodes. In cases of no suspicion on US, perioperative sentinel lymph node biopsy (SLNB) is undertaken [3] which, if negative, rules out disseminated disease with high accuracy [4]. If positive, the standard procedure is to perform axillary lymph node dissection (ALND) where all axillary lymph nodes are surgically removed. However, these procedures are invasive and may cause complications such as infection or seroma, and late effects as lymphedema, pain and shoulder impairment [5–7].

Currently, noninvasive preoperative staging of the axilla by MRI mammography is not recommended as routine, although macro-metastatic involvement of axillary lymph nodes is detectable in many cases. The morphological criteria for metastases include loss of the fatty hilum, size, eccentric cortical thickening, irregular margins, edema, and asymmetry [8,9] or dynamic contrast enhancement. Sensitivities for detecting metastatic lymph nodes using morphological criteria and dynamic features have previously been reported ranging from 50 % to 88 % [9–11] and cannot replace the need for histopathological verification [12]. Because of this, better noninvasive methods of staging the axilla are desired and should optimally be incorporable into whole-body imaging.

When lymph nodes become metastatic they are infiltrated by tumor cells and may lose their fatty hilum [13,14]. This means that fat content within the lymph node will be reduced while the increased cellularity increases the water content of the metastatic lymph node. Thus, the fat fraction (FF), will be decreased in metastatic lymph nodes. The Dixon MRI technique [15] can separate the water signal from the fat signal using multiple echoes yielding water (W), fat (F), in-phase (IP), and opposed-phase (OP) images [16]. From these images FF images can be calculated as F/IP [17] and the lymph node FF can be measured. FF from Dixon sequences are well established in measuring fat content in the liver [18].

However, the ability of FF to discriminate between metastatic and non-metastatic lymph nodes remains to be investigated. Since the axillary lymph nodes are small compared to the total volume of the liver, a high-resolution Dixon sequence with minimal motion artefacts are required to robustly calculate FF images in a lymph node. Ideally, the scan time used for such a sequence should be short enough to allow incorporation into clinical MRI mammography or whole-body MRI protocols. In the present study, we present the use of radial sampling to acquire high-resolution 3D Dixon images for lymph node FF quantitation. Radial sampling allows the acquisition of high-resolution 3D images in clinically feasible scan times and makes the sequence relatively motion robust.

The aim of the present study was to assess the diagnostic performance of lymph node FF from a high-resolution 3D radial Dixon sequence compared to conventional morphological parameters in breast cancer patients undergoing definitive surgery using histopathology as reference standard.

2. Material and methods

This prospective study was approved by the Central Denmark Region Committee on Health Research Ethics (reference number 1-10-72-425-17). Written informed consent was obtained prior to the patients' MRI examinations.

2.1. Patients

The eligibility criteria were women with biopsy verified primary or recurrent breast cancer referred for diagnostic work-up with whole-body MRI on a suspicion of disseminated disease. Indication for referral included advanced loco-regional disease, bone pain, weight loss, and fatigue. Eligible patients were identified at the Department of Plastic and Breast Surgery, Aarhus University Hospital prior to surgery and formed a consecutive cohort. After definitive surgery, histopathology of axillary lymph nodes was performed per our pathology department's standard.

2.2. MRI protocol

All patients were examined in the supine position on a 1.5 T whole-body MRI system with a DDAS spectrometer (Ingenia, release 5.3 software, Philips Medical Systems, Best, The Netherlands) using built-in posterior coil, dS HeadNeck coil, and Flex Coverage anterior coil from the scanner vendor. The patients received a whole-body MRI examination as part of their diagnostic work-up. In addition, a high-resolution 3D T1 gradient echo Dixon sequence was obtained centered over the patients' axillae. The following parameters were used: repetition time, (TR) 6.7 ms; echo time (TE) 1, 1.9 ms; TE2, 3.8 ms; flip angle, 10°; radial sampling, 220 %; slice thickness, 2 mm; gap, −1 mm; acquired voxel size, $1 \times 1 \times 2$ mm; reconstructed voxel size, $0.8 \times 0.8 \times 1$ mm; field of view, $400 \times 400 \times 150$ mm; number of signal averages, 1. The scan time of the axillary MRI examination was 5:21.

2.3. Post processing

FF images were calculated with the system software as F/IP. All four phases (F, W, IP, and OP) as well as FF images were transferred to a standalone workstation and analyzed using the Osirix Dicom viewer version 10 (Pixmeo, Bernex, Switzerland). All patient examinations were completely anonymized.

2.4. Image analysis

Assessment of the axillary lymph nodes was done in consensus by two radiologists with 4 (KS) and 3 years (TWB) of experience in body MRI. The readers were blinded to all clinical information and were without access to additional imaging data and the histopathological diagnosis of the patients' axillary lymph nodes. Morphological criteria were assessed on FF images. A lymph node was deemed metastatic on morphological MRI if it had loss of the fatty hilum or had at least two of the following criteria: eccentric cortical thickening, irregular margins, short axis > 10 mm, edema, or asymmetry [19]. On the FF images, an elliptical region of interest (ROI) was manually drawn in the cortex of the most suspicious lymph node (Fig. 1) as the size of the lymph nodes did not allow for whole lymph node segmentation. An elliptical ROI was chosen over other ROI shapes to include as many voxels of the lymph node cortex as possible while still maintaining a margin to the axillary fat. When placing the ROIs, special care was taken to avoid including the adjacent axillary fat as well as the fatty hilum as that would cause a falsely elevated FF measurement. In patients with no suspicious lymph nodes, the most representative lymph node was chosen for recording of morphological features and FF measurements. In addition, morphology and FF were measured in one benign appearing lymph node in the contralateral axilla for reference.

2.5. Statistical analysis

Normality of lymph node FFs was assessed visually using normal plots. All values are presented as mean ± standard deviation. A two-sample t-test was used to compare the mean FF of metastatic and non-metastatic lymph nodes. A receiver operating characteristics (ROC) curve analysis was performed on the ability of lymph node FF to differentiate between metastatic and non-metastatic lymph nodes. The optimal cut-off value was determined using the Youden index [20]. The sensitivity, specificity, positive predictive value (PPV), and negative
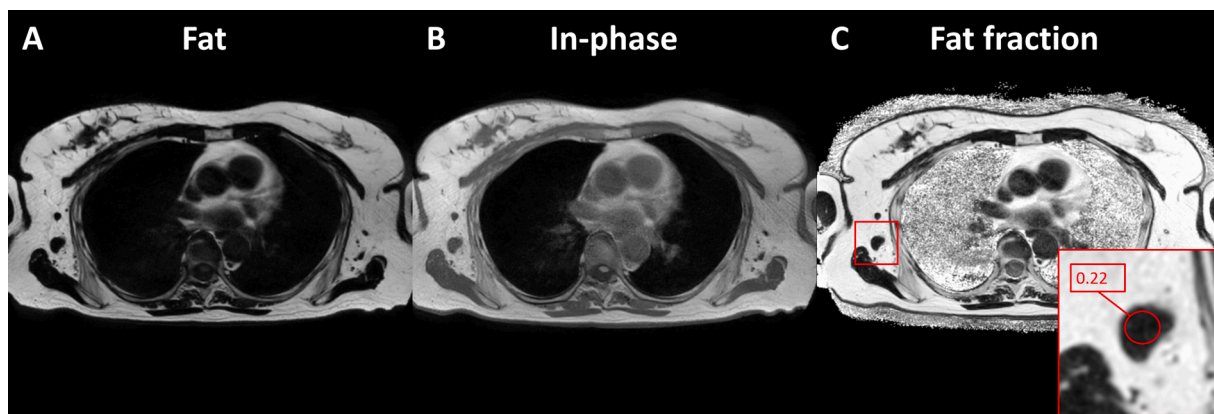
Fig. 1. Woman with a metastatic lymph node in her right axilla. The lymph node has lost its fatty hilum and has an FF of 0.22. (A) Fat phase, (B) in-phase, (C) FF image.

predictive value (NPV) based on the cut-off value were calculated using the histopathology report for verifying the nodal status. McNemar's test [21] was used to compare sensitivity and specificity of lymph node FF and morphological criteria. A p-value < 0.05 was considered statistically significant. All statistical analyses were done using STATA Statistics/Data analysis Special Edition version 16.1 (StataCorp, College Station, Texas).
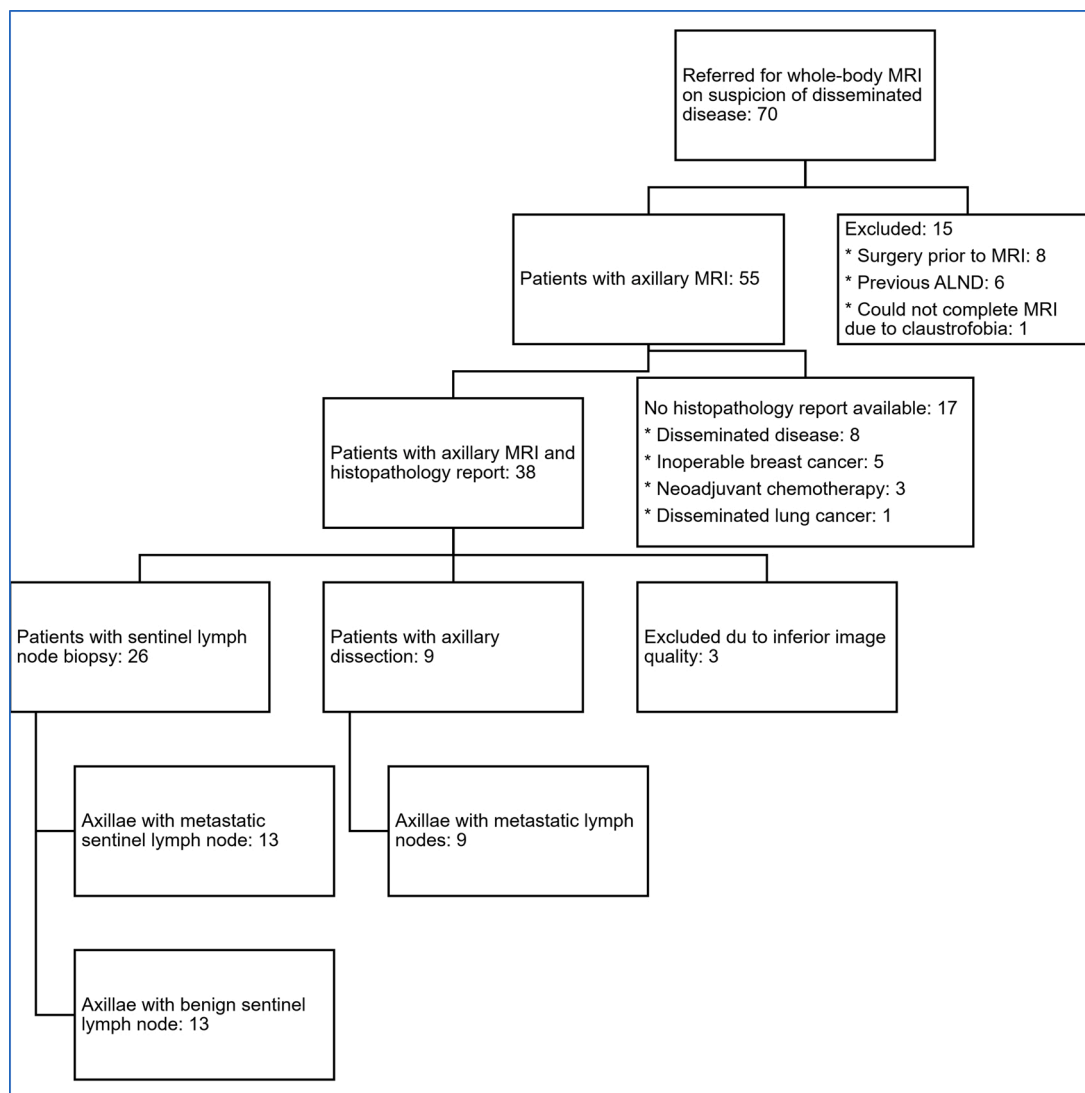

Fig. 2. Flow chart of the patient enrollment.

T.W. Buus et al.

European Journal of Radiology Open 7 (2020) 100284

3. Results

3.1. Patients

From April 2018 to November 2019, 70 eligible breast cancer patients were enrolled consecutively (Fig. 2). Of the 70 patients enrolled, 15 were excluded; 6 due to previous ALND, 8 due to surgery before MRI was performed and one because of claustrophobia. Of the remaining 55 patients, 17 patients did not undergo surgery and had no histology report (see Fig. 2). This left 38 patients with both axillary MRI and histopathology reports available for review. Three patients were excluded because of suboptimal axillary MRI due to motion artifacts and/or obesity making delineation of lymph nodes impossible. Of the final 35 patients, 26 had SLNB performed while 9 patients underwent ALND within 4 weeks after the MRI examination. 22 patients had histologically proven axillary lymph node metastases while the remaining 13 patients had benign histopathology. A total of 114 metastatic and 134 non-metastatic lymph nodes were excised (Table 1). The lymph node metastases were from invasive ductal carcinoma (IDC) (18/22), invasive lobular carcinoma (ILC) (1/22), combined IDC and ILC (2/22), and apocrine carcinoma (1/22). In one case occult invasive ductal carcinoma was suspected, as only ductal carcinoma in situ was found. One patient was diagnosed with micro-metastases only and was considered metastatic. The age of the patients was 60.2 ± 15.8 years.

3.2. Fat fractions

The metastatic lymph nodes had a mean lymph node FF of 0.20 ± 0.073. Non-metastatic lymph nodes had a mean lymph node FF of 0.31 ± 0.079 for ipsilateral lymph nodes, and 0.34 ± 0.15 for contralateral lymph nodes. Metastatic lymph node FF was significantly lower than that of ipsilateral non-metastatic (p < 0.001) and contralateral lymph nodes (p < 0.001) (Fig. 3). There were no significant differences between ipsilateral non-metastatic and contralateral lymph nodes (p = 0.52).

3.3. ROC analysis

On the ROC analysis, the area under the curve (AUC) for lymph node FF was 0.80 (Fig. 4). The best FF cutoff value for discriminating between non-metastatic and metastatic lymph nodes was 0.27, which yielded sensitivity 0.91, specificity 0.69, PPV 0.83, and NPV 0.82 for diagnosing

Table 1
Number of patients with SLNB or ALND and number of excised lymph nodes (LN).

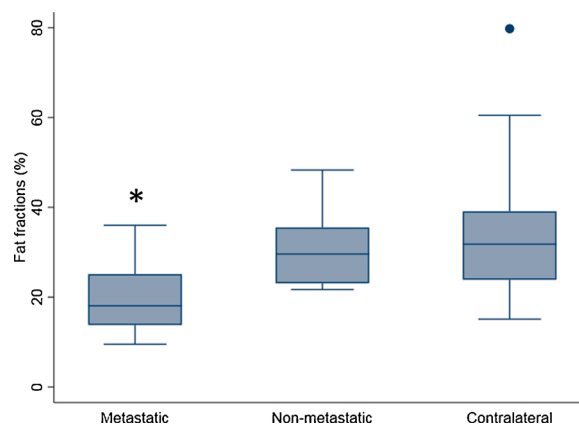|	SLNB			ALND		
Number of patients	26			9		
	Non-metastatic	Metastatic		Non-metastatic	Metastatic	
Number of axillae	13	13		0	9	
Number of lymph nodes	37	17		97	97	
		Macro	Micro		Macro	Micro
In total	37	15	2	97	85	12
LN from IDC	28	11	2	85	61	11
LN from ILC	3	0	0	12	24	1
LN from apocrine carcinoma	3	2	0	0	0	0
LN from combined IDC/ILC	3	2	0	0	0	0

Fig. 3. Box chart of FF in metastatic, non-metastatic and contralateral lymph nodes. Metastatic lymph node FF were significantly lower than both non-metastatic and contralateral lymph nodes as denoted by the *.
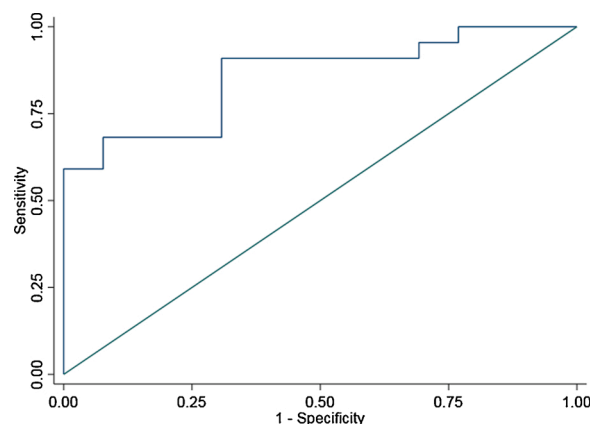

Fig. 4. ROC curve of lymph node FFs ability to discriminate between metastatic and non-metastatic lymph nodes.

metastatic lymph nodes. Morphological criteria yielded sensitivity 0.91, specificity 0.62, PPV 0.80, and NPV 0.80 for diagnosing metastatic lymph nodes with an AUC of 0.76. There were no significant differences between lymph node FF and morphological criteria for AUC (p = 0.29) or sensitivity and specificity (p = 0.71). Figs. 5 and 6 show examples of metastatic and non-metastatic lymph nodes correctly diagnosed by FF.

Combining lymph node FF and morphological criteria resulted in increased diagnostic performance; sensitivity 1.00, specificity 0.67, PPV 0.86, and NPV 1.00 with an AUC of 0.83.

4. Discussion

In the present study, we present the use of a high-resolution 3D radial Dixon sequence for detecting axillary lymph node metastases in breast cancer patients prior to surgery. The main findings of our study include a significantly reduced lymph node FF in metastatic lymph nodes and an increased sensitivity and NPV when combining morphological criteria with lymph node FF.

Lymph node FF from the Dixon sequence was significantly lower in metastatic lymph nodes compared to non-metastatic lymph nodes. The reduced fat content of the lymph nodes may be due to infiltrating tumor cells replacing intra-nodal fat. In addition to decreasing fat, the infiltrating tumor cells increases cellularity with increased water content as a result. This increase in cellularity has been shown to be measurable by MRI [22]. Both of these effects would contribute to the lower FF observed in metastatic lymph nodes.

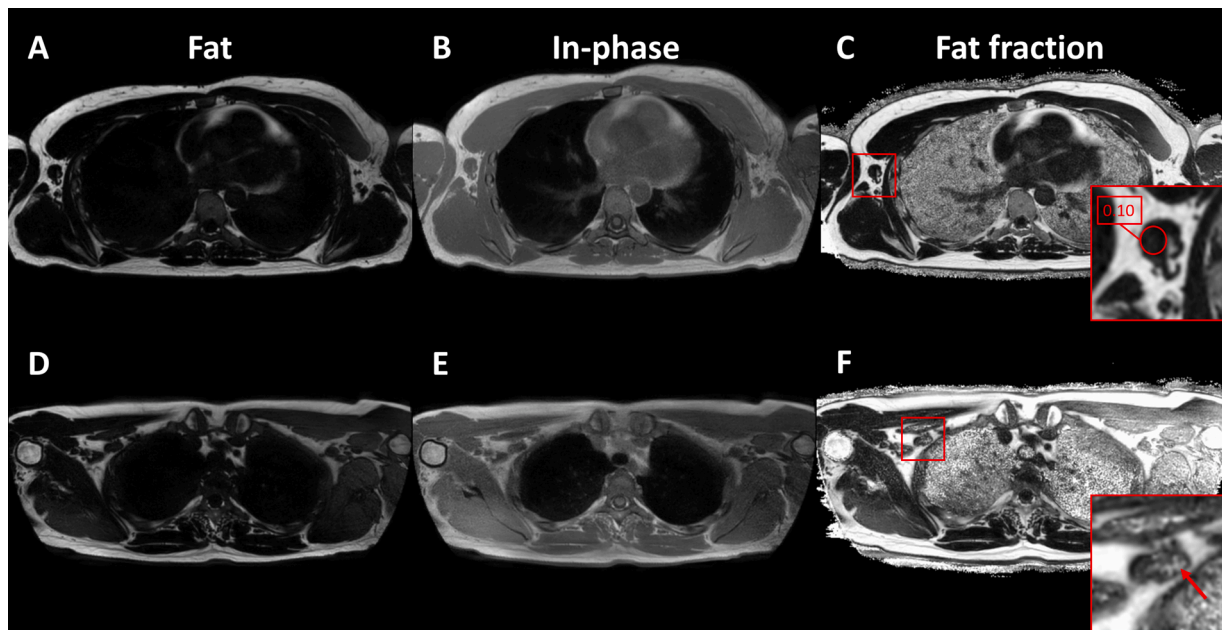In our study, morphological MRI had a sensitivity of 0.91 and

Fig. 5. (A-C) Woman with a histopathology report showing one metastatic lymph node in the right axilla. The lymph node (red box) has lost its fatty hilum, shows asymmetry, and cortical thickening and is correctly diagnosed as metastatic based on morphological criteria. The lymph node FF was 0.10 indicating metastasis. (D–F) Another woman with a histopathology report showing benign lymph nodes in the right axilla. The lymph node (red box) in the right axilla has lost its fatty hilum and has a short axis diameter > 10 mm and was falsely diagnosed as metastatic based on morphological criteria. The lymph node FF was 0.38 indicating benign histology. Also note the fat present inside the lymph node on the fat fraction image (red arrow).
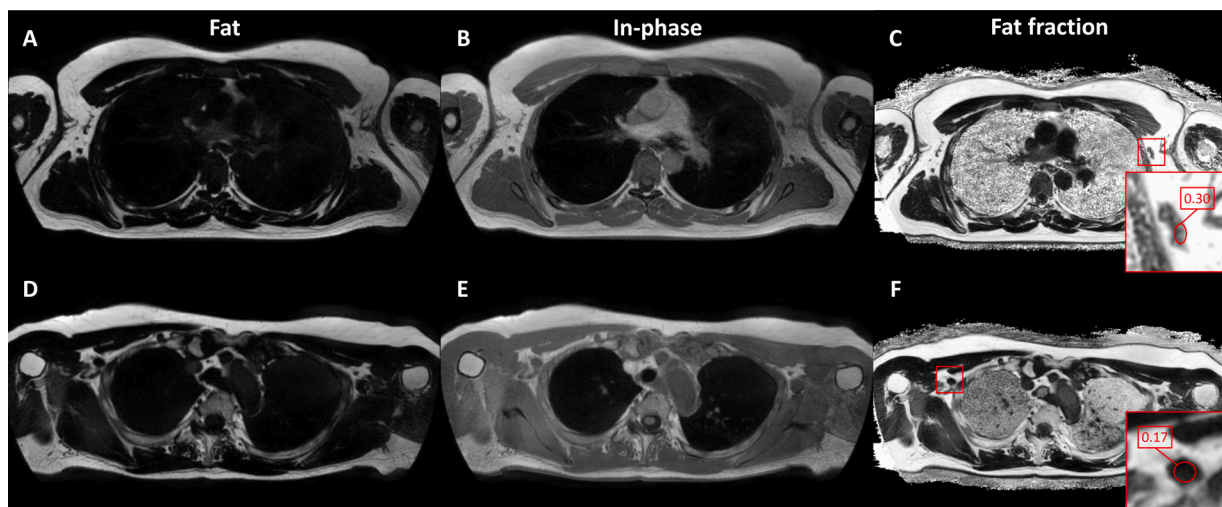

Fig. 6. (A-C) Woman with no metastatic lymph nodes on SLNB in the left axilla. The lymph node (red box) shows cortical thickening but still has its fatty hilum and is correctly diagnosed as non-metastatic based on morphological criteria. The lymph node FF was 0.30 indicating benign histology.
(D–F) Another woman with a histopathology report showing metastatic lymph nodes in the right axilla. The lymph node (red box) in the right axilla has lost its fatty hilum and shows asymmetry. It was correctly diagnosed as metastatic based on morphological criteria. The lymph node FF was 0.17 indicating metastasis.

specificity of 0.62. The sensitivity is higher than previously reported for detecting axillary lymph node metastases with MRI mammography [9, 10]. However, the specificity of morphological MRI was lower in our study. Since the AUC and diagnostic accuracy was similar between ours and previous studies, differences in sensitivity and specificity may be due to readers between studies having different thresholds for deeming a lymph node as metastatic. The sensitivity and specificity of lymph node FF were 0.91 and 0.69, respectively, with an AUC of 0.80. This was not significantly different from that of morphological criteria. However, when combining lymph node FF with morphological criteria the diagnostic performance increased with very high sensitivity and NPV. Even though we had few patients with no metastatic lymph nodes in our

study, the combination of lymph node FF and morphological criteria are promising for ruling out lymph node metastases. If confirmed in larger studies among multiple centers and across scanners from different vendors, this could potentially reduce the need for invasive diagnostic procedures in patients with morphologically unsuspicious lymph nodes and negative FF.

In two patients, lymph nodes that were falsely diagnosed as metastatic on morphological criteria were diagnosed correctly by lymph node FF. This was seen in large lymph nodes with no fatty hilum. Even though loss of fatty hilum [9,13,14] and the short axis diameter are two of the most important morphological criteria [9,23], the specificity is quite low. One patient with micrometastases only from SLNB was correctly

diagnosed as metastatic by lymph node FF but was falsely diagnosed as non-metastatic by morphological criteria. All other patients with micrometastases also had macrometastases, and since we only measured FF in the most suspicious lymph node, it is likely to have been in the ones containing macrometastases as they would appear most suspicious. While it was encouraging, that lymph node FF detected the one patient with micrometastases only, our patient population is too small to conclude on the ability of lymph node FF to detect micrometastases.

Among the strengths of our study, is the prospective study design and the use of a high-resolution 3D radial Dixon sequence allowing us to obtain FF images with voxels of $1 \times 1 \times 2$ mm without the use of dedicated breast coils. The spatial resolution and signal-to-noise ratio could potentially be improved further by using breast coils if obtained as part of MRI mammography. The Dixon sequence took 5:21 min and was robust across a patient population with a wide range of age and weight, making it realistic to implement into MRI mammography or whole-body MRI protocols.

Our study has some limitations. First, we did not attempt to correlate lymph nodes from the axillary MRI examination with the histopathology report on a node-to-node basis. Because of this, lymph nodes had to be correlated between MRI and histopathology on an axilla-to-axilla basis, as previously described by other authors [9,19,24]. Second, an elliptical ROI drawn in the lymph node cortex was chosen over a manual whole lymph node segmentation. Some of the lymph nodes were small, and even though the images had high-resolution, a whole lymph node segmentation would run the risk of adding partial volume from the adjacent axillary fat or fatty hilum. Since the FF measures fat, including even a small amount of the adjacent axillary fat within the ROI would cause falsely high FF. Because of this, the ROIs were drawn in the cortex with a safety margin to the axillary fat by the two radiologists in consensus by "eyeballing", and once drawn it was not moved. Third, even though our patients did receive a diffusion-weighted imaging (DWI) examination as part of whole-body imaging, we did not evaluate lymph node apparent diffusion coefficient (ADC) values from the DWI examination. This was due to our DWI protocol having low resolution (voxels of $4 \times 4 \times 6$ mm) with relatively low signal-to-noise ratio; mainly due to the use of short tau inversion recovery (STIR) fat suppression (as is recommended for whole-body DWI [25] instead of spectral attenuated inversion recovery (SPAIR) fat suppression used in MRI mammography DWI). DWI is another functional MRI technique that can be quantified through the ADC values. In two meta-analyses, Xing et al. [26] and Sui et al. [27] found sensitivities 0.83–0.89 and specificities 0.82–0.83 for ADC values to discriminate between metastatic and non-metastatic axillary lymph nodes with AUC 0.91–0.93. In our study, lymph node FF had a slightly higher sensitivity compared to the one reported for DWI but with a lower specificity. A combination of Dixon FF and DWI ADC values may further improve the discrimination between metastatic and non-metastatic lymph nodes. Finally, our study population was small and we only had 13/35 patients with benign histopathology. Since the patients were referred for whole-body imaging, the a priori risk of having lymph node metastases was increased in this patient cohort compared to the general patient population undergoing SLNB or ALND. However, sensitivity and specificity are, as opposed to the PPV and the NPV, independent of prevalence and should be unaffected by our small sample size.

5. Conclusions

In conclusion, lymph node FF from high-resolution 3D radial Dixon images are a promising quantitative indicator of metastases in axillary lymph nodes and may improve the ability of MRI to discriminate metastatic from non-metastatic lymph nodes. The Dixon sequence could potentially be incorporated into whole-body MRI and applied to lymph nodes in other parts of the body. Future studies should aim to validate lymph node FF on a node-to-node basis in vivo and ex vivo and examine ways of objective segmentation and ROI definition by e.g. using artificial intelligence techniques.

CRediT authorship contribution statement

Thomas Winther Buus: Conceptualization, Methodology, Formal analysis, Resources, Data curation, Writing - original draft, Visualization. **Kim Sivesgaard:** Investigation, Writing - review & editing. **Tanja Linde Fris:** Resources, Writing - review & editing. **Peer Michael Christiansen:** Conceptualization, Resources, Writing - review & editing. **Anders Bonde Jensen:** Conceptualization, Resources, Writing - review & editing, Supervision. **Erik Morre Pedersen:** Conceptualization, Methodology, Validation, Writing - review & editing, Supervision, Funding acquisition.

Declaration of Competing Interest

The authors report no declarations of interest.

Appendix A. Supplementary data

Supplementary material related to this article can be found, in the online version, at doi:https://doi.org/10.1016/j.ejro.2020.100284.

References

[1] F. Bray, J. Ferlay, I. Soerjomataram, R.L. Siegel, L.A. Torre, A. Jemal, Global cancer statistics 2018: GLOBOCAN estimates of incidence and mortality worldwide for 36 cancers in 185 countries, CA Cancer J. Clin. 68 (6) (2018) 394–424, https://doi.org/10.3322/caac.21492.

[2] D.N. Krag, S.J. Anderson, T.B. Julian, et al., Sentinel-lymph-node resection compared with conventional axillary-lymph-node dissection in clinically node-negative patients with breast cancer: overall survival findings from the NSABP B-32 randomised phase 3 trial, Lancet Oncol. 11 (10) (2010) 927–933, https://doi.org/10.1016/S1470-2045(10)70207-2.

[3] M. Fraile, M. Rull, F.J. Julián, et al., Sentinel node biopsy as a practical alternative to axillary lymph node dissection in breast cancer patients: an approach to its validity, Ann. Oncol. 11 (2000) 701–705, https://doi.org/10.1023/A:1008377910967.

[4] U. Veronesi, G. Viale, G. Paganelli, et al., Sentinel lymph node biopsy in breast cancer: ten-year results: of a randomized controlled study, Ann. Surg. 251 (4) (2010) 595–600, https://doi.org/10.1097/SLA.0b013e3181c0e92a.

[5] A. Soran, G. D'Angelo, M. Begovic, et al., Breast cancer-related lymphedema - What are the significant predictors and how they affect the severity of lymphedema? Breast J. 12 (6) (2006) 536–543, https://doi.org/10.1111/j.1524-4741.2006.00342.x.

[6] T. Ashikaga, D.N. Krag, S.R. Land, et al., Morbidity results from the NSABP B-32 trial comparing sentinel lymph node dissection versus axillary dissection, J. Surg. Oncol. 102 (2) (2010) 111–118, https://doi.org/10.1002/jso.21535.

[7] A. Lucci, L.M. McCall, P.D. Beitsch, et al., Surgical complications associated with sentinel lymph node dissection (SLND) plus axillary lymph node dissection compared with SLND alone in the American College of Surgeons Oncology Group trial Z0011, J. Clin. Oncol. 25 (24) (2007) 3657–3663, https://doi.org/10.1200/JCO.2006.07.4062.

[8] P.A.T. Baltzer, M. Dietzel, H.P. Burmeister, et al., Application of MR mammography beyond local staging: is there a potential to accurately assess axillary lymph nodes? Evaluation of an extended protocol in an initial prospective

study, Am. J. Roentgenol. 196 (5) (2011) 641–647, https://doi.org/10.2214/AJR.10.4889.

[9] E.J. Kim, S.H. Kim, B.J. Kang, B.G. Choi, B.J. Song, J.J. Choi, Diagnostic value of breast MRI for predicting metastatic axillary lymph nodes in breast cancer patients: Diffusion-weighted MRI and conventional MRI, Magn. Reson. Imaging 32 (10) (2014) 1230–1236, https://doi.org/10.1016/j.mri.2014.07.001.

[10] A.M. Scaranelo, R. Eiada, L.M. Jacks, S.R. Kulkarni, P. Crystal, Accuracy of unenhanced MR imaging in the detection of axillary lymph node metastasis: study of reproducibility and reliability, Radiology 262 (2) (2012) 425–434, https://doi.org/10.1148/radiol.11110639.

[11] R.-J. Schipper, M.-L. Paiman, R.G.H. Beets-Tan, et al., Diagnostic performance of dedicated axillary T2- and diffusion-weighted MR imaging for nodal staging in breast cancer, Radiology 275 (2) (2015) 345–355, https://doi.org/10.1148/radiol.14141167.

[12] S.J. Hyun, E.-K. Kim, H.J. Moon, J.H. Yoon, M.J. Kim, Preoperative axillary lymph node evaluation in breast cancer patients by breast magnetic resonance imaging (MRI): can breast MRI exclude advanced nodal disease? Eur. Radiol. 26 (2016) 3865–3873, https://doi.org/10.1007/s00330-016-4235-4.

[13] V.E. Mortellaro, J. Marshall, L. Singer, et al., Magnetic resonance imaging for axillary staging in patients with breast cancer, J. Magn. Reson. Imaging 30 (2) (2009) 309–312, https://doi.org/10.1002/jmri.21802.

[14] A.A.K.A. Razek, M.A. Lattif, A. Denewer, O. Farouk, N. Nada, Assessment of axillary lymph nodes in patients with breast cancer with diffusion-weighted MR imaging in combination with routine and dynamic contrast MR imaging, Breast Cancer 23 (2016) 525–532, https://doi.org/10.1007/s12282-015-0598-7.

[15] W.T. Dixon, Simple proton spectroscopic imaging, Radiology 153 (1) (1984) 189–194, https://doi.org/10.1148/radiology.153.1.6089263.

[16] H. Eggers, B. Brendel, A. Duijndam, G. Herigault, Dual-echo Dixon imaging with flexible choice of echo times, Magn. Reson. Med. 65 (1) (2011) 96–107, https://doi.org/10.1002/mrm.22578.

[17] S.B. Reeder, C. Sirlin, Quantification of liver fat with MRI, Natl. Inst. Heal. 18 (3) (2011) 337–357, https://doi.org/10.1016/j.mric.2010.08.013.

[18] H.K. Hussain, T.L. Chenevert, F.J. Londy, et al., Hepatic fat fraction: MR imaging for quantitative measurement and display – early experience, Radiology 237 (3) (2005) 1048–1055, https://doi.org/10.1148/radiol.2373041639.

[19] I. Guvenc, G.J. Whitman, P. Liu, C. Yalniz, J. Ma, B.E. Dogan, Diffusion-weighted MR imaging increases diagnostic accuracy of breast MR imaging for predicting axillary metastases in breast cancer patients, Breast J. 25 (2019) 47–55, https://doi.org/10.1111/tbj.13151.

[20] W.J. Youden, Index for rating diagnostic tests, Cancer 3 (1) (1950) 32–35, https://doi.org/10.1002/1097-0142(1950)3:1<32::AID-CNCR2820030106>3.0.CO;2-3.

[21] Q. McNemar, Note on the sampling error of the difference between correlated proportions or percentages, Psychometrika 12 (1947) 153–157, https://doi.org/10.1007/BF02295996.

[22] W. Junping, S. Tongguo, Z. Yunting, Y. Chunshui, B. Renju, Discrimination of axillary metastatic from nonmetastatic lymph nodes with PROPELLER diffusion-weighted MR imaging in a metastatic breast cancer model and its correlation with cellularity, J. Magn. Reson. Imaging 36 (3) (2012) 624–631, https://doi.org/10.1002/jmri.23695.

[23] A. Luciani, F. Pigneur, F. Ghozali, et al., Ex vivo MRI of axillary lymph nodes in breast cancer, Eur. J. Radiol. 69 (1) (2009) 59–66, https://doi.org/10.1016/j.ejrad.2008.07.040.

[24] J. Chung, J.H. Youk, J.-A. Kim, et al., Role of diffusion-weighted MRI: predicting axillary lymph node metastases in breast cancer, Acta radiol. 55 (8) (2014) 909–916, https://doi.org/10.1177/0284185113509094.

[25] A.R. Padhani, F.E. Lecouvet, N. Tunariu, et al., METastasis reporting and data system for prostate cancer: practical guidelines for acquisition, interpretation, and reporting of whole-body magnetic resonance imaging-based evaluations of multiorgan involvement in advanced prostate cancer, Eur. Urol. 71 (1) (2017) 81–92, https://doi.org/10.1016/j.eururo.2016.05.033.

[26] H. Xing, C.L. Song, W.J. Li, Meta analysis of lymph node metastasis of breast cancer patients: clinical value of DWI and ADC value, Eur. J. Radiol. 85 (6) (2016) 1132–1137, https://doi.org/10.1016/j.ejrad.2016.03.019.

[27] W.F. Sui, X. Chen, Z.K. Peng, J. Ye, J.T. Wu, The diagnosis of metastatic axillary lymph nodes of breast cancer by diffusion weighted imaging: a meta-analysis and systematic review, World J. Surg. Oncol. 14 (2016), https://doi.org/10.1186/s12957-016-0906-5.